Construction and Building Materials 76 (2015) 297–306

Contents lists available at ScienceDirect

Construction and Building Materials

journal homepage: www.elsevier.com/locate/conbuildmat

Optimizing the durability and service life of self-consolidating concrete containing metakaolin using statistical analysis

Ahmed A. Abouhussien *, Assem A.A. Hassan

Department of Civil Engineering, Faculty of Engineering and Applied Science, Memorial University of Newfoundland, St. John's, Newfoundland A1B 3X5, Canada

HIGHLIGHTS

- An optimum SCC mixture containing MK was determined and evaluated.
- The most significant factors affecting the chloride permeability were obtained.
- Linear relationship between RCPT and chloride diffusion coefficients was found.
- Prediction models for estimating the long-term properties of SCC were developed.
- Different percentages of decline of permeability versus time were warranted.

ARTICLE INFO

Article history:
Received 18 May 2014
Received in revised form 3 September 2014
Accepted 7 December 2014

Keywords:
Self-consolidating concrete
Metakaolin
Fly ash
Slag
Silica fume
Durability
Chloride permeability
Service life
Optimization
Statistical analysis

ABSTRACT

This paper utilizes the statistical design of experiments approach to optimize the mixture design of self-consolidating concrete (SCC) incorporating metakaolin (MK). The factors studied were total binder content, percentage of MK, water-to-binder ratio, and curing conditions. The results obtained from the developed statistical models were exploited to determine the most significant factors affecting the chloride permeability and the expected service life (calculated using Fick's second law of diffusion) of the tested mixtures. The developed models were also used to optimize the level of each response variable to minimize the chloride permeability, and to maximize the expected service life of the developed high performance SCC mixture. The results yielded an optimum SCC mixture with MK which achieved the lowest chloride permeability compared to counterpart SCC mixtures containing fly ash, slag, and silica fume. The results also showed that MK replacement proved to be the most significant variable affecting the chloride permeability, decline of permeability over time, and the service life of the tested mixtures.

1. Introduction

The production of self-consolidating concrete (SCC) is normally achieved by: (a) increasing the quantity of fines in the mixture, which could be done by incorporating one or more supplementary cementitious materials (SCM's) [1–3]; (b) adding high range water reducer admixtures (HRWRA), and if necessary, viscosity modifying admixtures (VMA) [4–5]; and/or (c) decreasing the coarse aggregate content in the mixture [6–7].

Different SCM's have been successfully used in the production of SCC, such as fly ash, ground granulated blast furnace slag, volcanic ash, cement kiln dust, rice husk ash, and silica fume [2]. Metakaolin (MK) is another type of SCM that is considered relatively new; it has been widely used for the production of high strength and high performance concrete over the past two decades [8]. In recent years, MK was introduced for the production of SCC. The behavior of MK in SCC mixtures was found to be similar to that in normal concrete mixtures, which showed an enhancement of the overall mechanical and durability performance [5].

Unfortunately, the production of SCC usually warrants a high cost, which is attributed to the high cement contents, high percentage of SCM's, and/or high doses of HRWRA. For this reason, optimizing SCC mixtures is vitally required to minimize the cost while maintaining the best fresh and hardened properties of the mixture. Statistical design of experiments is a useful tool that can be used to optimize the mixture components of SCC. Additionally, prediction models can be developed to evaluate the

* Corresponding author. Tel.: +1 709 330 6934.
E-mail address: aabouhussien@mun.ca (A.A. Abouhussien).

http://dx.doi.org/10.1016/j.conbuildmat.2014.12.010
0950-0618/

response at different levels of the governing factors. By using such models, the numerical optimization can then be performed to minimize or maximize the response [9–10]. Statistical design of experiments has been widely used in the mixture design and optimization for both normal concrete and SCC specially those containing SCM's [9–10]. Alternative soft computing methods are also applied to develop prediction models for different concrete properties. Examples of these methods are: artificial neural networks [11], genetic algorithm [12], and adaptive neuro-fuzzy inferencing systems [13]. However, most of these models require previous knowledge database about the input and output parameters along with significant mathematical work for the development of prediction relationships [13]. To this date, researchers apply the statistical design of experiments technique to analyze, model, study interaction between parameters, design, and optimize the behavior of SCC mixtures [14]. Durability and service life of concrete structures are considered to be the most important properties that need to be accounted for when optimizing SCC mixtures. Reinforced concrete structures, especially those subjected to high percentages of chlorides, should be given a special design consideration to extend their service life by reducing the corrosion of their embedded reinforcing steel [15–17]. The corrosion occurs when the chlorides from deicing salts, groundwater, or seawater penetrate the concrete cover and reach the reinforcing steel. Once the percentage of the chloride around the steel bar exceeds the threshold needed for corrosion initiation, the corrosion starts and rapidly propagates through the entire steel bar, leading to a mass loss and delamination of the concrete cover [17].

Chloride permeability is a significant property of concrete representing its service life. The assessment of the chloride permeability in concrete is usually performed using one of the following standard tests [18–19]: rapid chloride penetration test (RCPT) (ASTM C1202) and/or chloride bulk diffusion test (ASTM C1556). Most of the models used for predicting the corrosion initiation time account for the resistance of concrete to chlorides [16,20]. Concrete with low permeability and dense microstructure is proved to have more resistance to chloride ingress and longer time for corrosion initiation [17,21].

Recently, different methods were developed for predicting the service life of concrete structures. These methods usually monitor the service life of concrete structures in two periods, including initiation and propagation periods. The initiation period is the period in which the chlorides penetrate the concrete cover until they reach a threshold level (enough to initiate corrosion) at the rebar surface. The propagation period starts after the initiation period and ends when significant damage occurs in the structure resulting in cracks and rebar mass loss. The time of the initiation period is calculated using a simplified Fickian diffusion approach assuming that the chloride diffusion is the dominant mechanism of rebar corrosion. The time of the propagation period, however, depends on the definition of "significant damage." This level of damage in general varies depending on the requirements of the owner and the nature of the structure.

The main objective of this study was to develop an optimum SCC mixture incorporating metakaolin using a statistical design of experiments approach. The total binder content, percentage of MK, water-to-binder ratio, and curing conditions were varied to obtain the best mixture in terms of chloride permeability (RCPT and chloride diffusion), and extended service life. The statistical design of experiments approach was also used to present the most significant factors affecting each response variable in the mixture and to develop some prediction models for each test result. The study also presented a relationship between the different methods of assessing the chloride permeability in concrete for predicting the chloride diffusion of SCC mixtures containing metakaolin.

2. Research significance

Statistical prediction models can be used to predict the long-term behavior of SCC mixtures in terms of affecting variables. These models can be used to optimize the level of each variable and to minimize and/or maximize the responses of SCC mixtures. However, the available models in the literature are limited for SCC mixtures containing specific SCM's, such as FA, SF, and SG. As a result, a statistical optimization of SCC mixture containing MK was deemed necessary. The findings obtained from this investigation are of special interest for engineers applying MK in the production of SCC mixtures.

3. Experimental procedure

A total of 27 SCC mixtures were tested in this investigation. Twenty mixtures were used to optimize the mixture proportions of SCC using a statistical design of experiments approach, and 7 mixtures were used in the stage of validating the developed models. The 20 mixtures were designed by applying the Box–Wilson central composite design (CCD) method [22]. Three factors varied throughout the 20 mixtures, including the total binder content (A = 400–500 kg/m^3), water-to-binder ratio (B = 0.35–0.45), and the percentage of cement replacement by MK (C = 0–25%). The coarse-to-fine aggregate ratio was kept constant for all 20 mixtures as 0.9. The amount of HRWRA was determined based on maintaining a target slump flow of 650 ± 50 mm as per ASTM C1611 [23]. The slump flow diameter was fixed at this presumed value to ensure that all tested mixtures can achieve acceptable similar fresh properties for SCC. The amount of HRWRA required for each mixture to achieve the target slump flow was firstly determined based on testing some trial mixtures under similar mixing procedure. It should be noted that the HRWRA dosage was not considered as an independent variable in this study. The HRWRA dosage was only used to maintain a constant slump flow in all SCC mixtures. The reason behind that was if the HRWRA dosage was simultaneously varied as an independent factor with other mixtures ingredients, it would have yielded some unacceptable SCC mixtures with significantly varied values of slump flow.

After completing the fresh properties tests of the 20 mixtures, 100 mm (4 in) diameter × 200 mm (8 in) length cylinders were cast and cured for a maximum period of 180 days. These cylinders were used to prepare the samples of the RCPT and chloride diffusion tests. Two curing regimes were used: the first regime was to submerge the samples in water for 180 days, while the second regime was to store them in air for the whole 180-day period. Both regimes were performed at a controlled temperature of about 23 °C. After the 28-day curing period, the RCPT and chloride diffusion tests were performed on both air- and water-cured samples according to the standard tests ASTM C1202 [18] and C1556 [19], respectively.

The RCPT test was replicated at 90 and 180 days to measure the decrease in the chloride permeability versus concrete's age defined as the diffusion decay index (m). Using the values of m for each mixture and the chloride diffusion coefficients (D_a) obtained from the chloride diffusion test, the service life of the 20 mixtures were predicted by means of Fick's second law of diffusion.

A statistical analysis was performed on the results obtained from each test (RCPT and D_a tests), then the most significant factor affecting each response variable was determined, and prediction models for each test (response variable) were developed. The statistical analysis was completed by commercially available software for the design and analysis of experiments. These models were used to determine the optimum level of each factor by applying the numerical optimization tool.

The next stage used the numerical optimization tool to determine one optimum mixture proportions that achieved the best durability, and longest service life. In this stage, two SCC mixtures, including the optimum SCC mixture and another selected SCC mixture, were tested for validating the prediction models by comparing the results obtained from the models and the actual tests. Meanwhile, three additional SCC mixtures containing fly ash (FA), slag (SG), and silica fume (SF), as well as two normal concrete (NC) mixtures without any SCM's, were also tested and compared to the optimum SCC mixture.

3.1. Materials

In this program, type GU Canadian Portland cement, similar to ASTM Type I [24], with a specific gravity of 3.15, was used for both NC and SCC mixtures. The MK used in this research was delivered from the Eastern United States by Advanced Cement Technologies, conforming to ASTM C618 Class N [25], with a specific gravity of 2.56. The SG and SF used in this investigation have specific gravities of 2.89 and 2.27, respectively. FA conforming to ASTM C618 Class F [25] was employed in this project, with a specific gravity of 2.26. The chemical properties of cement and all SCM's are shown in Table 1.

A high range water reducer admixture (HRWRA), similar to ASTM Type F [26], was applied to achieve the required slump flow of SCC mixtures. The specific gravity, volatile weight, and pH of the HRWRA were 1.2, 62%, and 9.5, respectively. Natural sand was used for the production of the SCC mixtures with specific gravity of

Table 1
Chemical properties for SCM's and cement.

Chemical properties %	Cement	MK	SG	SF	FA
SiO_2	19.64	51–53	40.3	>85	52
Al_2O_3	5.48	42–44	8.4	–	23
Fe_2O_3	2.38	<2.2	0.5	–	11
FeO	–	–	–	<5	–
TiO_2	–	<3.0	–	–	–
C	–	–	–	<10	–
P_2O_5	–	<0.2	–	–	–
SO_4	–	<0.5	–	–	–
CaO	62.44	<0.2	38.71	<5	5
MgO	2.48	<0.1	11.06	<5	–
Na_2O	–	<0.05	–	–	–
C_3S	52.34	–	–	–	–
C_2S	16.83	–	–	–	–
C_3A	10.50	–	–	–	–
C_4AF	7.24	–	–	–	–
K_2O	–	<0.4	0.37	–	–
L.O.I.	2.05	<0.5	0.65	–	–

2.70 and water absorption of 1%. Both 10 mm and 20 mm maximum size natural crushed stones were included as coarse aggregates in the SCC mixtures with a specific gravity of 2.70 and water absorption of 1%.

3.2. Mixture design and SCC proportions using CCD method

The design of mixtures was obtained after determining the different levels of each factor by using the CCD method. This method divides the design space into three parts: the full-factorial part, the axial part, and the central part [22]. The three parts together yielded the 20 runs that were represented by 20 SCC mixtures included in the first stage of the study. The three parts consist of examining the studied factors at five different levels. The first part, the full-factorial, involved studying the three factors or variables ($k = 3$) at two levels only (-1 and $+1$ in coded factors) with a total number of runs of $n_f = 2^k = 8$ runs. Secondly, the axial part defined as $n_a = 2^k = 6$ runs and the coded factors were identified as the coded values of -1.68 and $+1.68$. The selection of the coded values of the axial part was designed to obtain a rotatable experimental design region, which can be achieved by using the value of $\alpha = \pm(2^k)^{1/4} = \pm 1.68$ [22]. By maintaining a rotatable design, the uncertainty of determined response surface symmetry can then be fixed. The remaining runs were set at the center, or $n_c = 6$, with a coded value of 0.

A minimum number of center points was calculated using the equation proposed by Schmidt and Launsby [22], $n_c = [4^*(n_f + 1)^{0.5}] - 2^k = 6$ runs. The coded values of each factor were calculated based on Eq. (1) for five different levels of each variable. For example, the coded value of water-to-binder ratio of 0.37 can be estimated by using Eq. (1) as follows: Coded Factor = $(0.37 - 0.4)/(0.5 * 0.06) = -1$. The overall range of variables was selected based on reviewing the literature of proportioning SCC containing metakaolin using similar material properties [5,27]:

$$\text{Coded Factor} = \frac{(\text{actual value} - \text{central value})}{0.5\ (\text{range between maximum and minimum values})} \quad (1)$$

The total number of runs (mixtures) was 20, as described above. By using the previously described levels of each factor for each mixture, the mixture proportions were calculated by applying the absolute volume method. Table 2 outlines the mixture proportions for each run (mixture). After determining the mixtures ingredients, all materials including cement, sand, SCM's, and coarse aggregate were dry mixed in a rotary mixer for 5 min. The required amounts of HRWRA (determined from the trial mixtures) were blended with the mixing water, then added to the dry materials and mixed for about 5 min. After achieving the target slump flow of SCC mixtures, the fresh properties tests were performed followed by casting samples from each mixture.

After analyzing the results of testing the 20 SCC mixtures, the numerical optimization was implemented and yielded the optimum SCC mixture containing MK. This optimum mixture (MK), along with another selected SCC mixture (MK-V), were then both tested under the same previously described tests for validating the statistical models obtained from the ANOVA. Furthermore, this optimum mixture was compared to three additional SCC mixtures (containing 30% FA, 30% SG, and 8% SF) and two NC mixtures (Table 2). The replacement levels of FA, SG, and SF were selected as the optimum levels for these SCM's based on the results obtained from other research [5,15,28]. Regarding the NC mixtures, two mixtures were included to examine different coarse aggregate sizes, denoted as NC1 (10 mm coarse aggregate) versus NC2 (20 mm coarse aggregate). The validation mixture containing MK (MK-V) was randomly selected to validate the statistical models.

4. Numerical procedure

4.1. Service life prediction using Fick's law of diffusion

After measuring the apparent chloride diffusion coefficients (D_a) and the diffusion decay index (m) for each mixture, the following assumptions were made to predict the service life for the tested mixtures:

- The chloride threshold value is 0.05% (% weight of concrete), as given from the literature [20,29].
- The chloride diffusion is the dominant mechanism and is governed by Fick's second law of diffusion in the differential Eq. (2) [30],

$$\frac{dC}{dt} = D_a \cdot \frac{d^2C}{dx^2} \quad (2)$$

where C = the chloride content, D_a = the apparent diffusion coefficient, x = the depth from the exposed surface, and t = time.

- The chloride diffusion coefficients (at 28 days) decrease periodically as a function of time because of the cement hydration process. As a result, the chloride diffusion should be calculated at different time periods using Eq. (3) [31]:

$$D(t) = D_{ref} \cdot \left(\frac{t_{ref}}{t}\right)^m \quad (3)$$

where $D(t)$ = diffusion coefficient at a time = t, D_{ref} = diffusion coefficient at time t_{ref} (28 days), and m = diffusion decay index.

- The surface chloride concentration (C_s) of the simulated structure had reached the maximum chloride concentration at the start time of chloride diffusion.

The solution for estimating the time of corrosion initiation was implemented using a finite difference application of Eq. (2). The values of chloride diffusion coefficient were varied at different time steps using Eq. (3), until the value of chloride concentration near the rebar surface reached the chloride threshold value. At this stage, the time was reported, which indicated the corrosion initiation for each mixture.

4.2. Statistical analysis and numerical optimization procedure

The results from each test were subjected to a statistical analysis using commercially available program for experimental design. This program performs nonlinear regression analysis for each test result (response variable) based on the input values (variables). Finally, the software yields a mathematical equation of the response. The developed equations are mostly based only on the most significant factors (variables) and their interactions. The equation can be linear or non-linear based on the behavior of the response variable throughout the range of variables. Linear equations involve main variables and their interactions, while non-linear formulas include higher order variables (quadratic). It should be noted that the linear models were firstly considered for some response variables as trial models (not presented in this paper) before choosing the CCD method. These linear models showed that the curvature had a significant effect on the response variables indicating that higher order variables were essentially utilized (using CCD method).

The significance of variables and their interactions was determined after performing the analysis of variance (ANOVA) by applying the least-square approach. The ANOVA tests the probability values (probability > F or P-value), which indicate the probability that the contribution of a given parameter to the tested response exceeds the value of the specified coefficient or the factor is significant if its value is <0.05. In addition, the degree of significance

Table 2
Mixture proportions for the 27 tested mixtures.

Mix. No.	A: total binder (kg/m^3)	B: water-to-binder	C: SCM level (%)	C.A. size (mm)	Cement (kg/m^3)	SCM (kg/m^3)	C.A. (kg/m^3)	F.A. (kg/m^3)	Water (kg/m^3)	HRWRA dose (l/m^3)	(HRWRA/total binder) × 100
1	420	0.37	19.9	10	336.42	83.58	868.45	964.94	155.4	10.43	2.48
2	480	0.37	5.1	10	455.52	24.48	822.98	914.42	177.6	4.00	0.83
3	450	0.40	12.5	10	393.75	56.25	828.88	920.98	180.0	4.57	1.02
4	450	0.40	12.5	10	393.75	56.25	828.88	920.98	180.0	4.57	1.02
5	480	0.43	19.9	10	384.48	95.52	781.10	867.89	206.4	4.86	1.01
6	450	0.45	12.5	10	393.75	56.25	801.18	890.19	202.5	3.29	0.73
7	450	0.35	12.5	10	393.75	56.25	856.59	951.77	157.5	15.43	3.43
8	400	0.40	12.5	10	350.00	50.00	873.63	970.70	160.0	8.14	2.04
9	420	0.37	5.1	10	398.58	21.42	874.05	971.17	155.4	8.71	2.07
10	450	0.40	25.0	10	337.50	112.5	823.82	915.35	180.0	7.33	1.63
11	420	0.43	19.9	10	336.42	83.58	837.41	930.46	180.6	6.14	1.46
12	450	0.40	12.5	10	393.75	56.25	828.88	920.98	180.0	5.29	1.18
13	480	0.43	5.1	10	455.52	24.48	787.50	875.00	206.4	2.57	0.54
14	420	0.43	5.1	10	398.58	21.42	843.02	936.68	180.6	3.57	0.85
15	450	0.40	12.5	10	393.75	56.25	828.88	920.98	180.0	4.71	1.05
16	450	0.40	12.5	10	393.75	56.25	828.88	920.98	180.0	4.57	1.02
17	480	0.37	19.9	10	384.48	95.52	816.57	907.30	177.6	9.57	1.99
18	500	0.40	12.5	10	437.50	62.50	784.14	871.27	200.0	4.29	0.86
19	450	0.40	12.5	10	393.75	56.25	828.88	920.98	180.0	5.29	1.18
20	450	0.40	0.0	10	450.00	0.00	833.95	926.62	180.0	2.33	0.52
MK	490	0.39	19.9	10	392.3	97.657	795.85	884.27	191.1	10.77	2.20
MK-V	450	0.40	15.0	10	382.5	67.5	827.87	919.86	180.0	5.29	1.18
SG	490	0.39	30.0	10	343	147	799.47	888.31	191.1	1.54	0.31
FA	490	0.39	30.0	10	343	147	782.01	868.90	191.1	2.00	0.41
SF	490	0.39	8.0	10	450.8	39.2	798.70	887.45	191.1	3.08	0.63
NC1	490	0.39	0.0	10	490	0	804.65	894.05	191.1	–	–
NC2	490	0.39	0.0	20	490	0	804.65	894.05	191.1	–	–

Note: C.A. and F.A. are coarse and fine aggregates, respectively; MK-V = validation SCC mixture containing MK; 1 kg/m^3 = 1.65 Ib/yd^3; 1 mm = 0.039 in.

among the significant factors can be determined based on the *F*-value for each factor. The factor with a higher *F*-value is considered more significant than other factors with lower *F*-values. On this basis, the significant variables for each response variable were selected to form the prediction equations. As a result, only variables with *P*-value of less than or equal 0.05 were considered significant and included in the model, and those had *P*-value higher than 0.05 were excluded. These equations exhibit some coefficients, which depend on the contribution of each variable. The equations can be interpreted in forms of coded values or actual values of significant variables. The factor with lower value of probability > *F* is preceded by higher coefficients in the respective equation (only in case of equations in the form of coded values are used). For simplifying the equations, the form of actual values of each variable was applied for models, in this paper. The selection of these equations was limited to obtaining a possible higher value of correlation coefficient R^2 for each model. After many trials in the utilized software, best-fit models were then obtained for each response. These fitted models were tested to check the normality of the residuals, detect the presence of autocorrelation in the residuals, and detect regression outliers which may influence fitting the model to the data. It should be mentioned that the diagnostics tool in the utilized software was used to test the prediction models. These tests involved checking normal plot of residual, residuals versus predicted and run values, residual versus three individual factors, and predicted versus actual values plots. Moreover, Box-Cox plots for Power Transforms were used to check if any transformation is required in the prediction model. The results of these tests showed that after trying different forms of power transforms, the natural log transformation was recommended for all prediction models described in this paper. In addition, after performing the natural log transformations, all fitted models yielded satisfactory diagnostics results and deemed useful for prediction.

Upon obtaining the prediction equation for every response, the numerical optimization tool was exploited to determine the optimum level of each factor (*A*, *B*, and *C*). The numerical optimization was performed as a multiple-response optimization developed by Derringer and Suich, described by Myers, Montgomery and Anderson-Cook [32]. The developed prediction models were used in this optimization, along with the predefined targets or the optimization constraints, in a number of trials, which maintained the desired criteria. The optimization was then performed by choosing the limits to determine the area that gives the optimal zone superimposed. The target in this technique was established to maximize the corrosion initiation times, and to minimize the chloride permeability of the SCC mixture. In this optimization, the developed prediction models were used, along with the predefined targets or the optimization constraints, in a number of trials which maintained the desired criteria.

5. Results and discussions

Fresh properties tests were conducted to measure the flow ability/viscosity (T_{500}, T_{500J}, and V-funnel), passing ability (difference between slump and J-ring flow diameters, and L-box), and segregation (segregation factor) of all tested mixtures, and the results obtained from each test are presented in Table 3. It can be noticed from Table 3 that all tested SCC mixtures achieved the presumed target slump flow (650 ± 50 mm). Nevertheless, some mixtures showed relatively low passing ability (L-Box), low J-Ring, and high V-Funnel values compared with those recommended by the European guidelines for SCC [33]. However, theses mixtures were used for optimization purposes and may still also be used for specific SCC applications such as ramps, walls, and piles [33]. The fresh properties tests were followed by testing the hardened and durability properties of the 27 tested mixtures, which are presented in Table 4.

5.1. Rapid chloride permeability test (RCPT)

An ANOVA analysis was completed for both results obtained from air- and water-curing samples to select the most significant factors affecting the 28-days, 90-days, and 180-days RCPT.

Table 3
Results of the fresh and hardened properties for the 27 tested mixtures.

Mix. No.	Slump flow (mm)	T_{500} (s)	J-ring flow (mm)	T_{500} J-ring (s)	Slump-J-ring (mm)	V-funnel (s)		S_f[†]	L-box ratio H2/H1	Air (%)	28-Days f_c' (MPa)	
						Initial	Final				Air	Water
1	629	9.5	604	13.5	25	40	63	0.58	0.65	1.7	70.3	74.8
2	640	2.5	605	4.5	35	30	48	0.60	0.55	1.6	73.5	74.0
3	610	3.2	580	5.5	30	24	40	0.67	0.67	2.3	74.1	76.5
4	650	3.7	621	5.8	29	26	43	0.65	0.69	2.1	75.8	77.8
5	653	2.0	641	3.0	12	5	6	0.20	0.93	3.3	64.1	72.5
6	625	2.5	605	3.7	20	4	5	0.25	0.77	2.4	62.0	67.3
7	673	5.5	636	8.6	37	34	59	0.74	0.50	1.5	77.7	78.3
8	635	7.2	600	9.3	35	32	55	0.72	0.52	1.8	60.9	62.1
9	600	8.5	560	11.8	40	36	89	1.47	0.45	2	51.1	54.1
10	662	4.5	645	5.6	17	30	45	0.50	0.78	1.8	72.8	79.9
11	650	4.7	634	6.2	16	34	48	0.41	0.83	1.4	62.6	68.9
12	640	3.5	615	4.4	25	22	35	0.59	0.60	1.8	73.6	79.1
13	673	1.5	659	2.3	14	3.5	4.5	0.29	0.69	1.4	54.7	61.1
14	625	3.8	604	6.5	21	8	13	0.63	0.68	1.2	49.3	58.1
15	640	4.2	610	5.9	30	23	38	0.65	0.64	1.7	70.9	77.8
16	635	4.0	603	5.3	32	29	46	0.59	0.59	1.9	73.1	80.2
17	653	6.5	625	8.25	28	24	36	0.50	0.80	0.9	78.6	82.3
18	625	3.3	605	3.9	20	10	13	0.30	0.70	1.9	78.1	82.2
19	635	4.5	608	5.8	27	27	45	0.67	0.66	2.0	75.9	81.9
20	625	3.0	592	4.0	33	15	34	1.27	0.55	2.0	55.3	57.0
MK	650	3.5	632	4.0	18	8	11	0.38	0.80	1.0	74.7	82.1
MK-V	655	3.3	625	4.5	30	22	33	0.50	0.69	1.5	72.2	81.2
SG	667	2.2	628	3.3	39	6	9	0.50	0.70	0.9	42.4	54.3
FA	650	3.0	622	3.5	28	7	10	0.43	0.77	1.4	50.1	66.0
SF	635	2.0	570	6.0	65	7.5	13	0.73	0.63	1.2	62.1	71.4
NC1	85[*]	–	–	–	–	–	–	–	–	2.0	54.1	62.7
NC2	170[*]	–	–	–	–	–	–	–	–	1.7	51.1	57.5

Note: 1 mm = 0.039 in; 1 MPa = 145 psi.
[*] Slump height in NC mixtures.
[†] Segregation factor.

Meanwhile, the prediction models for the RCPT values were obtained in the logarithmic form of the total charge passed in the RCPT. The model in Eq. (4) predicts the 28-days RCPT of air-curing samples. In this model, the most important variables were C, C^2, B, B^2, A, and A^2 (respectively in order of significance), with $R^2 = 0.97$. Alternatively, the model for water-curing samples included only C, C^2, B, A as the most significant factors, respectively, with ($R^2 = 0.98$), as seen in Eq. (5).

$$\text{Ln 28-days RCPT (air curing)} = 55.75 - 0.104A - 122.66B - 0.31C + 0.000111A^2 + 163.98B^2 + 0.0086C^2 \ \text{(Coulombs)} \quad (4)$$

$$\text{Ln 28-days RCPT (water curing)} = 8.37 - 0.0022A + 2.55B - 0.294C + 0.0076C^2 \ \text{(Coulombs)} \quad (5)$$

Similarly, the prediction models for the 90- and 180-days RCPT were developed for both air- and water-cured samples. These equations are based on the most significant factors governing the 90- and 180-days RCPT values. These significant factors are C, C^2, B, B^2, and A, respectively in order of significance, as shown in Eqs. (6)–(9) ($R^2 = 0.97$; $R^2 = 0.99$; $R^2 = 0.96$; and $R^2 = 0.98$, respectively).

$$\text{Ln 90-days RCPT (air curing)} = 34.199 - 0.00364A - 129.68B - 0.276C + 172.723B^2 + 0.0069C^2 \ \text{(Coulombs)} \quad (6)$$

$$\text{Ln 90-days RCPT (water curing)} = 19.84 - 0.0013A - 58.55B - 0.261C + 76.66B^2 + 0.0059C^2 \ \text{(Coulombs)} \quad (7)$$

$$\text{Ln 180-days RCPT (air curing)} = 35.818 - 0.003A - 140.59B - 0.26C + 187.13B^2 + 0.0062C^2 \ \text{(Coulombs)} \quad (8)$$

$$\text{Ln 180-days RCPT (water curing)} = 20.971 - 0.0007A - 67.49B - 0.24C + 88.73B^2 + 0.005C^2 \ \text{(Coulombs)} \quad (9)$$

5.1.1. Effect of mixture proportions on the RCPT

The prediction models show that all three tested factors (A, B, and C) had a significant effect on the RCPT values for both air- and water-cured samples. The MK replacement (factor C) was found to be the most significant factor influencing the RCPT reading, followed by water-to-binder ratio (factor B) and total binder (factor A), respectively. The effect of MK replacement on the RCPT was found to be 2.5 and 4.0 times greater than that of water-to-binder ratio and total binder content, respectively. This result may be attributed to the additional consumption of calcium hydroxide in MK mixtures thus reducing the OH^- ions and eventually decrease the RCPT values [5].

The results shown in Table 4 show that increasing the binder content from 420 to 480 kg/m^3 resulted in an average reduction of 20% in the RCPT reading (indicating a lower chloride permeability) of air- and water-cured samples. This reduction was expected from increasing the total binder material in the mixture, which resulted in more hydration product to fill the gaps in the concrete microstructure and eventually decreased the concrete permeability. This effect of binder content matched that obtained from similar statistical models from other research performed on SCC containing fly ash [9]. It should be noted that the increase in cement content is also expected to increase the RCPT values as the OH^- ions (calcium hydroxide) increases with higher cement content; however, the densification of the mixture microstructure as a result of formation of more hydration products appeared to have a greater effect on reducing the RCPT values. Increasing the water-to-binder ratio from 0.37 to 0.43 showed a counter effect on the RCPT of SCC. This increase yielded an average increase of approximately 30% in the RCPT in the air- and water-cured samples. It should be noted that using relatively high water-to-binder ratios resulted in an increase of the capillary pores, which led to higher permeability of the concrete.

As mentioned earlier, the MK replacement was seen as the most significant factor affecting the RCPT of SCC mixtures. As the MK percentage increased from 5.1% to 19.9%, the RCPT results were significantly decreased by nearly 75% in both air- and water-cured samples. These results indicated the superior effect of MK in minimizing the chloride permeability of SCC regardless of the curing type. It should be noted that the addition of higher replacements of MK (>20%) showed higher RCPT values; as a result, 20% of MK replacement was deemed the optimum percentage. It can also be seen from Table 4 that minimum RCPT values were obtained from mixture number 17 (A = 480 kg/m^3, B = 0.37, and C = 19.9%), which had the maximum compressive strength. On the contrary, the maximum RCPT was related to mixture number 20 (A = 450 kg/m^3, B = 0.4, and C = 0%), which had no MK (0%). This result manifests the effect of MK in reducing the chloride permeability of SCC.

5.1.2. Effect of curing on the RCPT

Table 4 indicates that an identical trend was obtained from the chloride permeability of both air- and water-cured samples. However, the water-cured samples showed lower permeability than air-cured ones throughout the 20 SCC mixtures containing MK. The 20 tested mixtures showed that air-cured samples had an average of 21% higher RCPT values than that of their water-cured counterparts. The results of the 90- and 180-days tests are shown and compared to the 28-days counterparts, as seen in Table 4.

It is clear from the table that all mixtures exhibited a significant decrease in the RCPT values from 28 to 180 days, as expected. These results were attributed to the effect of the hydration process during the curing period, which decreased the permeability of the concrete.

Although the 20 mixtures had an almost identical trend of decline of permeability versus time, different percentages of reduction based on the mixture proportions were warranted for each mixture. These percentages of change are represented by the factor called a diffusion decay index (m). This factor is an important property of the concrete as it is used in the service life prediction models; for example, the model presented in the Life-365 software [31]. These models consider using this factor to represent the change in the chloride permeability over time [16,20,31].

The factor m was found to be affected by the mixture proportions, including binder content, water-to-binder ratio, and incorporating SCM's [16,34]. The factor m was calculated for the 20 mixtures using Eq. (10) [8,16,34] for both air- and water-cured samples based on the assumption that the change in the RCPT values is almost linear with the curing time in the logarithmic scales (Table 4). The values of the m factor for the 20 SCC mixtures containing MK ranged between 0.065 and 0.374. The absolute minimum and maximum m values were obtained from mixtures number 6 (A = 450 kg/m^3, B = 0.45, and C = 12.5%) and 10 (A = 450 kg/m^3, B = 0.4, and C = 25%), respectively. Minimum values of 0.065 and 0.083 were obtained from mixture number 6 when cured in air and water, respectively. These values may be attributed to the highest water-to-binder ratio used in this mixture (0.45). The maximum m values were 0.371 and 0.374 and were associated with mixture number 10 in air- and water-cured samples, respectively. These maximum m values were warranted, owing to the highest MK replacement level used in this mixture (25%). It should be noted that mixture number 20 (A = 450 kg/m^3, B = 0.4, and C = 25%) had the same binder content and water-to-binder ratio as that of mixture number 10 but did not contain MK. As a result, this mixture had lower m values than mixture number 10 (0.263 versus 0.371). The values of m obtained from this test were used in calculating the change in the chloride diffusion coefficients and eventually the corrosion initiation times for the 20 SCC mixtures.

$$\mathrm{RCPT} = \mathrm{RCPT}_{ref} \cdot \left(\frac{T_{ref}}{T}\right)^m \tag{10}$$

where RCPT = the RCPT reading at any time T, T = target time of prediction, RCPT_{ref} = RCPT at the time T_{ref}, and T_{ref} = time at which *RCPT* reading is known (28 days).

It should be noted that some results from literature suggested that the chloride diffusion test is more accurate than the RCPT [35–36], thus calculating m using the former would be recommended. However, the comparison performed by Zeljkovic [8] showed in most tested mixtures that both tests yielded similar values of m. These results were further confirmed from the linear relationship obtained between the RCPT values and the apparent chloride diffusion coefficients presented in Section 5.6.

5.2. Chloride diffusion coefficient (D_a)

Apparent chloride diffusion coefficient (D_a) at the age of 28 days was measured experimentally as a part of the bulk chloride diffusion test. The prediction models that relate the coefficient D_a with the most important factors affecting it for both air and water curing are presented in Eqs. (11) and (12) (R^2 = 0.94 and R^2 = 0.95, respectively). As seen in Eq. (11), the factors that mostly affected the air-cured coefficient D_a were C, B, C^2, BC, and A, respectively in order of significance. On the other hand, the factors C, C^2, B, B^2, and A were the most significant effects governing the water-cured coefficient D_a, respectively in order of significance (Eq. (12)). The influence of the MK percentage on D_a showed to be 2 and 4.5 times higher than that of water-to-binder ratio and total binder content, respectively. These results matched the impact of the three variables (MK percentage, water-to-binder ratio, and total binder content) on the RCPT values.

$$\begin{aligned}\text{Ln 28-days } D_a \text{ (air curing)} &= 10.368 - 0.0048A - 2.78B - 0.67C \\ &\quad + 1.144 \cdot B \cdot C + 0.0055C^2 \ (\times 10^{-14}\ \mathrm{m^2/s})\end{aligned} \tag{11}$$

$$\begin{aligned}\text{Ln 28-days } D_a \text{ (water curing)} \\ = 33.795 - 0.0048A - 128.71B - 0.266C + 167.92B^2 \\ + 0.0064C^2 \ (\times 10^{-14}\ \mathrm{m^2/s})\end{aligned} \tag{12}$$

5.3. Corrosion initiation times

The corrosion initiation periods for the 20 SCC mixtures were calculated for each curing type, as shown in Fig. 1. It is clear from the figure that different mixture proportions and curing procedures significantly affected the time for corrosion to start (initiation period). Moreover, a wide range of the initiation periods was obtained from the 20 SCC mixtures (1.7–65.1 years). This wide range manifests the effect of the durability performance of the SCC on the corrosion initiation time and the overall service life of structures.

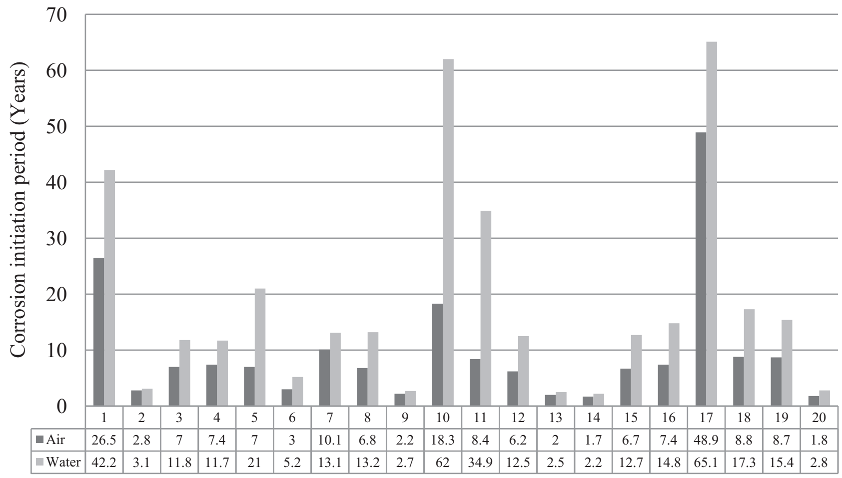

Fig. 1. Corrosion initiation periods for the 20 SCC mixtures containing MK.

Table 4
Results of the durability properties for the 27 tested mixtures.

Mix. No	28-Days RCPT (Coulombs)		90-Days RCPT (Coulombs)		180-Days RCPT (Coulombs)		m		28-Days D_a ($\times 10^{-12}$ m^2/s)	
	Air	Water	Air	Water	Air	Water	Air	Water	Air	Water
1	329	293	258	210	209	169	0.244	0.296	1.01	0.89
2	1156	1132	1091	1044	939	894	0.112	0.127	4.24	4.01
3	400	341	367	315	326	290	0.110	0.087	1.82	1.04
4	390	365	358	335	325	302	0.098	0.102	1.65	1.11
5	571	288	470	247	402	221	0.189	0.142	2.37	0.78
6	760	439	704	398	673	376	0.065	0.083	3.57	2.22
7	361	329	346	315	300	272	0.099	0.102	1.25	0.99
8	542	356	482	327	394	275	0.171	0.139	2.29	1.15
9	2066	1518	1627	1188	1480	1081	0.179	0.182	6.05	5.26
10	451	315	277	193	226	157	0.371	0.374	2.24	0.95
11	678	345	462	232	402	197	0.281	0.301	2.76	1.06
12	412	367	371	332	335	300	0.111	0.108	2.05	1.07
13	1948	1319	1832	1228	1628	1105	0.096	0.095	5.74	4.57
14	2649	1597	2395	1441	2124	1293	0.119	0.113	6.97	5.38
15	407	373	365	334	324	295	0.123	0.126	1.98	1.13
16	405	327	360	290	318	257	0.130	0.129	1.85	0.99
17	280	240	218	187	185	159	0.223	0.221	0.55	0.42
18	388	351	326	294	305	276	0.129	0.129	1.58	0.87
19	397	347	352	307	295	259	0.160	0.157	1.79	1.08
20	3987	3739	3173	2842	2446	2024	0.263	0.330	8.43	7.29
MK	268	217	248	196	203	166	0.149	0.144	0.58	0.43
MK-V	378	311	315	264	283	239	0.155	0.140	1.58	1.14
SG	1715	1120	1572	584	1325	320	0.139	0.673	2.46	1.16
FA	2450	1325	1954	378	1632	208	0.218	0.995	3.80	1.23
SF	1180	509	705	431	425	268	0.549	0.344	0.78	0.69
NC1	2773	2309	2267	1957	1925	1760	0.196	0.146	4.72	3.96
NC2	3396	2614	2680	2087	2450	1825	0.175	0.193	6.17	5.33

Note: 1 m^2/s = 1550 in^2/s.

5.3.1. Effect of curing on corrosion initiation times

As seen in Fig. 1, all water-cured samples showed higher initiation times than their air-cured counterparts. This trend was expected given the lower chloride permeability of water-cured samples than air-cured ones in the chloride diffusion test. Nevertheless, the differences in the corrosion initiation times between air- and water-cured samples were not constant for all SCC mixtures. The maximum difference was 43.7 years and was obtained in mixture number 10 (A = 450 kg/m^3, B = 0.4, and C = 25%), which had the maximum replacement level of MK. This difference was attributed to the higher effect of curing on the mixtures containing high percentages of MK. In this mixture, water curing decreased the chloride diffusion coefficient from 2.24×10^{-12} to 9.54×10^{-13}, which significantly affected the initiation times. Significant differences (>10 years) were also obtained from mixtures number 1, 5, 11, and 17. These mixtures were cast with 19.9% MK replacement. On the other hand, the minimum difference was 0.3 years and was given by mixture number 2 (A = 480 kg/m^3, B = 0.37, and C = 5.1%), which exhibited the lower percentage of MK (5.1%). This result indicated that increasing the MK percentage greatly increased the difference between air- and water-cured samples.

5.3.2. Effect of SCC mixture proportions on corrosion initiation times

It can be noticed from Fig. 1 that different corrosion initiation periods were associated with different SCC mixtures. These results were expected as the 20 mixtures exhibited various D_a, which represents the most important factor in the corrosion process. As a result, the mixture with the minimum diffusion coefficients was mixture number 17 (A = 480 kg/m^3, B = 0.37, and C = 19.9%), which yielded the maximum corrosion initiation periods (48.9 and 65.1 years for air and water curing respectively). Meanwhile, the mixture with the minimum corrosion initiation periods (1.7 and 2.2 years for air and water curing, respectively) was mixture number 14 (A = 420 kg/m^3, B = 0.43, and C = 5.1%). It should be noted that mixture number 20 (A = 450 kg/m^3, B = 0.4, and C = 0%) was expected to show the minimum corrosion initiation time owing to its highest D_a (maximum among all 20 mixtures). However, the diffusion decay index (m), which also plays a significant role in the corrosion initiation time, was higher in mixture number 20 compared to mixture number 14 (0.33 versus 0.113). This decrease in the diffusion decay index (m) caused a shorter corrosion initiation time in mixture number 14 compared to mixture number 20.

5.4. Optimization of SCC mixture and models validation

By reviewing the results of the 20 mixtures, the optimum mixture in terms of fresh properties (Table 3) appeared to be mixture number 5 (A = 480 kg/m^3, B = 0.43, and C = 19.9%) owing to its high flow ability (T_{500}, T_{500J}, and V-funnel), low segregation factor, and superior passing ability (lowest difference between slump and J-ring flow diameters and highest L-box ratio). Meanwhile, the optimum mixture in terms of hardened and durability properties (Tables 3 and 4) appeared to be mixture number 17 (A = 480 kg/m^3, B = 0.37, and C = 19.9%) owing to its highest compressive strength, lowest chloride permeability, and longest corrosion initiation time. These two mixtures both had a binder content of 480 kg/m^3 and an MK percent of 19.9%. It is clear that the mixture with high water-to-binder ratio (0.43) had the optimum fresh properties (mixture number 5), as expected. Moreover, the mixture with low water-to-binder ratio (0.37) had the maximum strength and the minimum chloride permeability/diffusion (mixture number 17). However, in order to determine one mixture achieving the balance of the optimum fresh properties, strength, durability, and service life, the numerical optimization tool was utilized. This tool is available with the method of central composite design (CCD) in the commercially used software.

The results of this optimization yielded an optimum SCC mixture having the following ingredients: A (total binder = 490 kg/m^3), B (W/B = 0.39), and C (MK ratio = 19.9%). This optimum mixture and another validation mixture were tested under the same procedure to validate the prediction models (Table 5). It can be seen that the results obtained from the prediction models are relatively close to the actual test results. However, it is can be seen from Table 5 that some response variables exhibit relatively high differences (10–20%) between the predicted and tested values. These differences may be attributed to local defects in the tested samples or change in curing temperatures. These discrepancies were expected from the results of tests like RCPT and chloride diffusion specially for testing RCPT samples up to 6 months. These prediction models can be ideally acceptable for obtaining mixture properties to achieve a presumed range of chloride permeability. For example, it can be applied to obtain high, moderate, low, very low, or negligible chloride ion penetrability as per ASTM C1202 [18].

5.5. Comparison of the optimum SCC mixture containing MK, other SCM's mixtures, and NC mixtures

The optimum SCC mixture containing MK obtained previously from the numerical optimization process was tested and compared to counterpart mixtures containing other SCM's. The results from the fresh and hardened properties tests are described in Tables 3 and 4, while the RCPT results at 28-, 90-, and 180-days are shown in Table 4. The minimum charge passed (RCPT) was found in the MK mixture, which indicated the minimum chloride permeability in both air- and water-cured samples. Meanwhile, SF had the second lowest RCPT after the MK mixture, followed by SG and FA, respectively. It is also clear from Table 4 that all SCC mixtures had lower RCPT values compared to NC mixtures. This result manifested the effect of using SCM's in reducing the chloride permeability of SCC and highlighted the superior behavior of the optimized MK SCC mixture compared to the NC mixture in both the compressive strength and chloride permeability. On the other hand, NC mixtures demonstrated different RCPT values based on the coarse aggregate size. For example, NC2 had slightly higher RCPT values than NC1 due to the bigger coarse aggregate size used in NC2 compared to NC1 (20 mm versus 10 mm). This result shows that the increase in coarse aggregate size resulted in higher RCPT values.

The effect of curing on the RCPT of SCC and NC mixtures can be clearly observed from Table 4. All water-cured samples showed to have lower RCPT values compared to their counterparts cured in air. In addition, a longer curing period decreased the RCPT coulombs for both air- and water-cured samples (Table 4). However, in some cases the effect of water curing was shown to be more dominant than the effect of the length of the curing period. For example, in SG, FA, SF, and NC2 the 28 days RCPT of water-cured samples was lower than the 93 days RCPT of the same samples cured in air.

The apparent chloride diffusion coefficients for the six selected mixtures were measured as a part of the bulk chloride diffusion test for air- and water-cured samples (Table 4). As expected, MK had the minimum chloride diffusion coefficients in both air- and water-cured samples. Meanwhile, the NC2 had the absolute maximum chloride diffusion factors (6.17×10^{-12}, 5.33×10^{-12} m^2/s) for both air- and water-cured samples. In addition, all water-cured samples attained lower chloride diffusion coefficients compared to air-cured counterparts. It is worth noting that, however, the above comparison involved using SCC mixtures containing percentages of FA, SG, and SF that were not optimized in this investigation (obtained from the literature). As a result, the comparison is only valid for SCC mixtures containing the selected percentages of these different SCM's.

5.6. Relationship between RCPT and chloride diffusion coefficients

Similar to RCPT, the D_a coefficient also represents the permeability of concrete. For this reason, showing that a relationship

Table 5
Validation of the statistical models.

Mix. No.	28-Days RCPT (Coulombs)		90-Days RCPT (Coulombs)		180-Days RCPT (Coulombs)		28-Days D_a ($\times 10^{-12}$ m^2/s)	
	Air	Water	Air	Water	Air	Water	Air	Water
MK (predicted)	299	239	217	187	180	157	1.01	0.54
MK (tested)	268	217	248	196	185	160	0.88	0.43
MK-V (predicted)	360	299	310	248	289	217	1.72	0.87
MK-V (tested)	378	311	315	264	283	239	1.58	1.14

Note: 1 m^2/s = 1550 in^2/s.

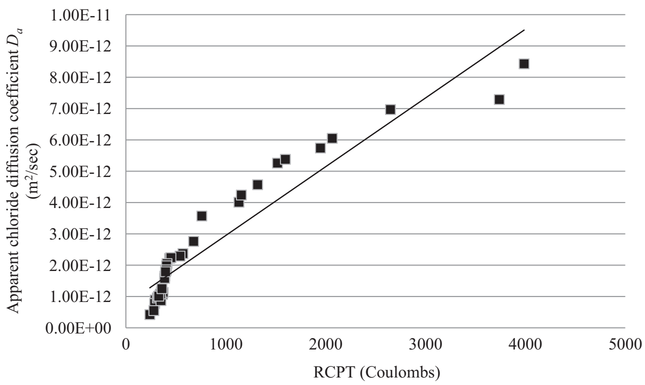

Fig. 2. Relationship between D_a and RCPT for air- and water-cured samples.

existed between the RCPT and the D_a was deemed necessary. Fig. 2 shows the relationship between the RCPT and the apparent chloride diffusion coefficient for the 20 SCC mixtures at 28 days. It is obvious from the figure that an almost linear relationship exists between the RCPT and the chloride diffusion tests. This relationship was confirmed from the results obtained by similar studies performed on high-performance concretes containing silica fume and slag [35]. On the other hand, earlier studies on several mortar and concrete mixtures with fly ash, silica fume, slag, and HRWRA showed poor correlation between RCPT and diffusion tests [36–37]. As a result, a linear equation was developed to predict the coefficient D_a by substituting the RCPT value. This equation can be used for a quick estimation of the chloride diffusion coefficient using the RCPT procedure, which requires only 6 h instead of 35 days to complete. Eq. (13) can be utilized to estimate the D_a for air- and water-cured samples as a function of the RCPT (coulombs) for the SCC mixtures ($R^2 = 0.9$).

It should be noted that this equation can only be used as a quick estimation for SCC mixtures containing MK with all other ingredients lying in the tested range of this paper.

$$\text{28-days } D_a = 7.522 \cdot 10^{-13} + 2.196 \cdot 10^{-15} \cdot \text{RCPT } (\text{m}^2/\text{s}) \qquad (13)$$

6. Conclusions

The analysis and discussion of the results from the experimental tests and statistical analysis were completed and the following conclusions were drawn:

1. The MK replacement (factor C) had the most significant effect on the chloride permeability (RCPT and D_a), followed by water-to-binder ratio (factor B), and then the total binder content (factor A), respectively. The effect of MK on the chloride permeability (as the averages of the results of RCPT and chloride diffusion) was found to be 2.25 and 4.25 times greater than that of water-to-binder ratio and total binder content, respectively.
2. All tested mixtures witnessed an almost linear trend of decline of permeability versus time; however, different percentages of reduction were warranted based on the mixture proportions. The MK replacement was found to be the most significant factor affecting this reduction, followed by the total binder content and water-to-binder ratio, respectively.
3. An optimum SCC with lowest chloride permeability, and longest corrosion initiation time showed to contain a total binder of 490 kg/m^3, water-to-binder ratio of 0.39, and replacement of MK by 19.9%.
4. Comparing the optimum SCC mixture containing MK to those containing FA, SF, SG, and NC mixtures showed that the 20% MK mixture exhibited the lowest chloride permeability, followed by 8% SF, 30% FA, 30% SG, NC1, and NC2, respectively.
5. The results of all the tested mixtures showed a linear relation between the RCPT values and the chloride diffusion coefficients, regardless of the mixture proportions or curing conditions. From this result, a linear relationship was developed and can be used to estimate the chloride diffusion coefficients in a relatively shorter amount of time by using the results obtained from the RCPT test.
6. Testing validation mixtures and comparing the results from the prediction models manifested the usefulness of these models for estimating the long-term properties of SCC mixtures containing MK.

References

[1] Khayat KH. Workability, testing, and performance of self-consolidating concrete. ACI Mater J 1999;96(3):346–53.
[2] Lachemi M, Hossain KMA, Lambros V, Bouzoubaâ N. Development of cost-effective self-consolidating concrete incorporating Fly Ash, slag cement, or viscosity-modifying admixtures. ACI Mater J 2003(5):419–25.
[3] Russell HG. ACI defines high-performance concrete. Concr Int 1999;21(2):56–7.
[4] Khayat KH. Optimization and performance of air-entrained, self-consolidating concrete. ACI Mater J 2000;97(5):526–35.
[5] Hassan AAA, Hossain KMA, Lachemi M. Effect of metakaolin and silica fume on the durability of self-consolidating concrete. Cement Concr Compos 2012;34(6):801–7.
[6] Khayat KH, Manai K, Trudel A. In situ mechanical properties of wall elements using self-consolidating concrete. ACI Mater J 1997;94(6):491–500.
[7] Lachemi M, Hossain KMA, Lambros V. Shear resistance of self-consolidating concrete beams – experimental investigation. Can J Civil Eng 2005;32(6):1103–13.
[8] Zeljkovic M. Metakaolin effects on concrete durability [Master's thesis]. Canada: Department of Civil Engineering, University of Toronto; 2009, 163 pp.
[9] Patel R, Hossain KMA, Shehata M, Bouzoubaâ N, Lachemi M. Development of statistical models for mixture design of high-volume Fly Ash self-consolidating concrete. ACI Mater J 2004;101(4):294–302.
[10] Sonebi M. Applications of statistical models in proportioning medium-strength self-consolidating concrete. ACI Mater J 2004;101(5):339–46.
[11] Ghafoori N, Najimi M, Sobhani J, Aqel MA. Predicting rapid chloride permeability of self-consolidating concrete: a comparative study on statistical and neural network models. Constr Building Mater J 2013;44:381–90.
[12] Jayaram MA, Nataraja MC, Ravikumar CN. Elitist genetic algorithm models: optimization of high performance concrete mixes. Mater Manuf Process 2009;24:225–9.
[13] Tesfamariam S, Najjaran H. Adaptive network-fuzzy inferencing to estimate concrete strength using mix design. J Mater Civil Eng 2007;19:550–60.
[14] Ghafari E, Costa H, Júlio E. RSM-based model to predict the performance of self-compacting UHPC reinforced with hybrid steel micro-fibers. Constr Building Mater J 2014;66:375–83.
[15] Hassan AAA, Hossain KMA, Lachemi M. Corrosion resistance of self-consolidating concrete in full-scale reinforced beams. Cement Concr Compos 2009;31(1):29–38.
[16] Boddy A, Bentz E, Thomas MDA, Hooton RD. An overview and sensitivity study of a multimechanistic chloride transport model. Cement Concr Res 1999;29(6):827–37.
[17] Hooton RD, Geiker MR, Bentz EC. Effects of curing on chloride ingress and implications on service life. ACI Mater J 2002;99(2):201–6.
[18] ASTM C1202-97. Standard test method for electrical indication of concrete's ability to resist chloride ion penetration. West Conshohocken, PA: ASTM International; 1997. 7 pp..
[19] ASTM C1556-11a. Standard test method for determining the apparent chloride diffusion coefficient of cementitious mixtures by bulk diffusion. West Conshohocken, PA: ASTM International; 2011. 7 pp..
[20] Ehlen M, Thomas MDA, Bentz EC. Widely used software helps assess uncertainties in concrete service life and life-cycle costs. ACI Concr Int 2009;31(5):41–6.
[21] Sujjavanich S, Sida V, Suwanvitaya P. Chloride permeability and corrosion risk of high-volume Fly Ash concrete with mid-range water reducer. ACI Mater J 2005;102(3):177–82.
[22] Schmidt SR, Launsby RG. In: Kiemele MJ, editor. Understanding industrial designed experiments, 4th ed.. Colorado Springs, CO: Air Academic Press; 1994. p. 1–48.
[23] ASTM C1611-09be1. Standard test method for slump flow of self-consolidating concrete. West Conshohocken, PA: ASTM International; 2009. 6 pp..

[24] ASTM C150–12. Standard specification for portland cement. West Conshohocken, PA: ASTM International; 2012. 9 pp..

[25] ASTM C618–12a. Standard specification for coal Fly Ash and raw or calcined natural pozzolan for use in concrete. West Conshohocken, PA: ASTM International; 2012. 5 pp..

[26] ASTM C494/C494M-13. Standard specification for chemical admixtures for concrete. West Conshohocken, PA: ASTM International; 2013. 10 pp..

[27] Vejmelková E, Keppert M, Rovnaníková P, Ondrácek M, Keršner Z. Properties of high performance concrete containing fine-ground ceramics as supplementary cementitious material. Cement Concr Compos 2012;34(1): 55–61.

[28] Sadok H, Kenai A, Courard L, Darimont A. Microstructure and durability of mortars modified with medium active blast furnace slag. Constr Building Mater 2011;25(2):1018–25.

[29] Trejo D, Pillai RG. Accelerated chloride threshold testing: part I - ASTM A615 and A706 reinforcement. ACI Mater J 2003;100(6):519–27.

[30] Gjørv OE. Durability and service life of concrete structures. Proceedings 6, The First fib Congress, Japan Prestressed Concrete Engineering Association, Tokyo. p. 1–16.

[31] Bentz EC, Thomas MDA. Life-365 TM service life prediction model™ and computer program for predicting the service life and life-cycle cost of reinforced concrete exposed to chlorides. Version 2.1, user manual, 2012. 80 pp..

[32] Myers RH, Montgomery DC, Anderson-Cook CM. Response surface methodology: process and product optimization using designed experiments. 3rd ed. New York: Wiley Series in Probability and Statistics; 2009.

[33] EFNARC. The European guidelines for self-compacting concrete specification, production and use. English ed. Norfolk, UK: European Federation for Specialist Construction Chemicals and Concrete Systems; 2005. 63 pp..

[34] Nokken M, Boddy A, Hooton RD, Thomas MDA. Time dependent diffusion in concrete: three laboratory studies. Cement Concr Res 2006;36(1):200–7.

[35] Hooton RD, Titherington MP. Chloride resistance of high-performance concretes subjected to accelerated curing. Cement Concr Res 2004;34:1561–7.

[36] McGrath PF, Hooton RD. Re-evaluation of the AASHTO T259 90-day salt ponding test. Cement Concr Res 1999;29:1239–48.

[37] Scanlon MJ, Sherman MR. Fly Ash concrete: an evaluation of chloride penetration testing methods. ACI Concr Int 1996;18(6):57–62.